

Enhanced Molecular CO₂ Electroreduction Enabled by a Flexible Hydrophilic Channel for Relay Proton Shuttling

Caroline K. Williams, Amir Lashgari, Jingchao Chai, and Jianbing "Jimmy" Jiang*[a]

The effects of primary and second coordination spheres on molecular electrocatalysis have been extensively studied, yet investigations of third functional spheres are rarely reported. Here, an electrocatalyst (ZnPEG8T) was developed with a hydrophilic channel as a third functional sphere that facilitates relay proton shuttling to the primary and second coordination spheres for enhanced catalytic CO₂ reduction. Using foot-ofthe-wave analysis, the **ZnPEG8T** catalyst displayed CO₂-to-CO activity (TOF_{max}) thirty times greater than that of the benchmark catalyst without a third functional sphere. A kinetic isotopic effect (KIE) study, in conjunction with voltammetry and UV/Vis spectroscopy, uncovered that the rate-limiting step was not the protonation step of the metallocarboxylate intermediate, as observed in many other molecular CO2 reduction electrocatalysts, but rather the replenishment of protons in the proton-shuttling channel. Controlled-potential electrolysis using ZnPEG8T displayed a faradaic efficiency of 100% for CO_2 -to-CO conversion at -2.4 V vs. Fc/Fc⁺. A Tafel plot was also generated for a comparison to other reported molecular catalysts. This report validates a strategy for incorporating higher functional spheres for enhanced catalytic efficiency in proton-coupled electron-transfer reactions.

Incorporation of second coordination spheres into the ligand frameworks of molecular catalysts has led to the successful development of many electrocatalysts for hydrogen evolution,[1] oxygen reduction, [2] formate oxidation, [3] carbon dioxide (CO₂) reduction, [4] and water oxidation. [5] Pre-positioned second coordination spheres have been proposed to increase the turnover number/frequency and lower the overpotentials through stabilization of catalytic intermediates.^[6] In catalytic CO₂ reduction, the catalyst-CO₂ adduct, typically a metallocarboxylate, is stabilized through local proton donors (phenols, triazole, imidazole, and carboxylic acids), [4c,e-h] proton-shuttling channels (urea),[4d] and hydrogen-bonding networks (amines)[4b] in the second coordination sphere and oxygen atom in the metallocarboxylate intermediate, or through-space electrostatic interactions between positively charged units, such as ammonium, in the second coordination sphere and the negatively charged metallocarboxylate intermediate. [7] Although CO₂ itself can function as an oxygen acceptor,^[8] the presence of protons lowers the overpotential by protonation-promoted C—OH cleavage.^[4b] Given that a sufficient number of protons facilitate CO₂ reduction, whereas an excess results in undesirable hydrogen evolution reactions, investigation of the proton delivery mechanism is vital for enhanced catalytic efficiency. In reported CO₂ reduction studies, great attention has been paid to primary coordination environments (types of metal centers and ligands),^[3,4f,8,9] second coordination spheres (position, acidity, hydrophobicity, etc.),^[4,10] electrolyte systems,^[11] and electrode materials.^[9d,12] Studies on the effects of third and higher functional spheres on molecular catalytic activity are rarely reported.^[13]

In our previous report on a zinc porphyrin electrocatalyst (ZnC8T), we observed synergistic effects of triazole units as a second coordination sphere for enhanced catalytic CO2 conversion efficiency.[14] The eight protonated triazole units form a picket-fence hydration shell on each side of the porphyrin plane, facilitating intramolecular protonation of the metallocarboxylate intermediate. Herein, to understand the proton-shuttling mechanism and evaluate the structure-function relationship to optimal proton concentration, a new porphyrin, **ZnPEG8T**, was designed with a built-in hydrophilic channel to facilitate relay proton shuttling to the second coordination sphere for protonation of the metallocarboxylate intermediate. This novel design decouples the hydrogen bonding/protonation and relay proton-shuttling steps to facilitate mechanistic studies. The ligand framework also allows for discrete control over the second coordination sphere and higher-sphere proton-shuttling channel without affecting the first coordination environment. A kinetic isotopic effect (KIE) study, in conjunction with voltammetry and UV/Vis spectroscopy, uncovered that the rate-limiting step is not the protonation step of the metallocarboxylate intermediate, as observed in many other molecular CO₂ reduction electrocatalysts, [4a, 15] but rather the replenishment of protons in the proton-shuttling channel. This work represents the first example of a pendant hydrophilic channel in a molecular catalyst facilitating relay proton shuttling for improved catalytic CO₂ efficiency and provides new insights into a handful of proton-coupled electron-transfer reac-

Compared to the benchmark catalyst, **ZnC8T**, having eight hydrophobic *n*-octyl chains, catalyst **ZnPEG8T** bears a hydrophilic poly(ethylene glycol) (PEG) chain on each of its eight triazole units (Figure 1). A "click reaction" of octaethynylporphyrin with 1-azido-2-[2-(2-methoxyethoxy)ethoxy]ethane (PEG3 azide) in the presence of copper(I) afforded **ZnPEG8T** in a 65% yield. A control compound bearing the same eight PEG chains without triazole units (**ZnPEG0T**) was also prepared (Figure 1,

Supporting Information and the ORCID identification number(s) for the author(s) of this article can be found under: https://doi.org/10.1002/cssc.202001037.

[[]a] C. K. Williams, A. Lashgari, Dr. J. Chai, Prof. J. Jiang Department of Chemistry University of Cincinnati P.O. Box 210172, Cincinnati, Ohio 45221 (United States) E-mail: jianbing.jiang@uc.edu

Figure 1. Structures of the ZnPEG8T, ZnC8T, and ZnPEG0T electrocatalysts.

see the Supporting Information for synthesis details). All compounds were purified and characterized (¹H NMR spectroscopy, UV/Vis spectroscopy, and MS) prior to redox property and electrocatalytic studies.

The electrochemical properties of **ZnPEG8T** were studied by using cyclic voltammetry (CV) in anhydrous DMF with 0.1 м tetrabutylammonium hexafluorophosphate (TBAPF₆) under an argon atmosphere. Three successive one-electron reduction peaks were observed at -1.75, -2.1, and -2.3 V vs. Fc/Fc⁺ (Figure 2). The first redox event was reversible, whereas the second and third were quasi-reversible. CVs at various scan rates (10-300 mV s⁻¹) were performed under the same conditions (Figure 2). The linear relationship between the peak currents at -1.75 V vs. Fc/Fc⁺ and the square roots of the scan rates (Figure 2, inset) indicates a diffusion-controlled process according to the Randles–Sevcik equation. $^{[4a,15]}$ The CV behavior of ZnPEG8T and the triazole-free compound ZnPEG0T (Figure S4 in the Supporting Information) is nearly identical to that of previously reported **ZnC8T**,^[14] suggesting that incorporation of triazole or PEG units does not impose any significant electronic effects on the electrochemical properties of the zinc porphyrin framework.

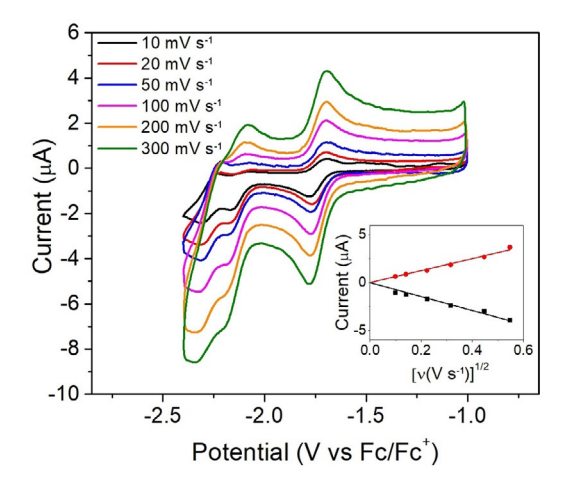


Figure 2. Scan-rate-dependent CVs of 0.5 mm ZnPEG8T in DMF with 0.1 m TBAPF $_{\!6}.$

The catalytic properties of ZnPEG8T were also studied by CV. The catalytic current (i_{cat}) at -2.4 V vs. Fc/Fc⁺ was normalized to the non-catalytic peak current (i_p) of the first electron reduction of each catalyst. A current increase ($i_{cat}/i_p = 3.3$) at the second redox peak was observed when measured under saturated CO₂ (0.23 M)^[4c] in anhydrous DMF compared to argon atmosphere (Figure 3 A). This current increase is attributed to CO2 reduction under aprotic conditions, in which CO2 functions as an oxygen acceptor,[8] even though this process is thermodynamically unfavorable.[17] The addition of water (5 M) to the catalytic system provided an even larger increase in current ($i_{cat}/i_p = 31.0$) and shifted the catalytic potential to the first reduction peak, suggesting an electron-transfer step followed by an irreversible chemi-

cal reaction step.^[18] The onset potential was approximately 300 mV lower than that under proton-free conditions, indicative of energetically favored proton-assisted CO₂ reduction.

The normalized catalytic currents for ZnC8T and ZnPEG0T, under the same catalytic conditions, are 19.4 and 10.9, respectively, indicating that ZnPEG8T is a more active catalyst than its PEG-free and triazole-free analogues (Table S2 in the Supporting Information contains i_{cat}/i_p for all catalysts). Different scan rates of the ZnPEG8T catalyst were attempted to reach pure kinetic conditions for CV.[18a,b] Unfortunately, an S-shaped CV trace was not achieved, even though the catalytic activity of all three catalysts was found to be independent of scan rate (Figures S5-S7 in the Supporting Information). To estimate kinetic information, the maximum turnover frequency (TOF_{max}) was calculated by using foot-of-the-wave analysis (FOWA). [18a,b] Based on Equation S1 in the Supporting Information, TOF_{max} for ZnPEG8T was calculated to be 1843 s⁻¹, which is thirty times greater than those of ZnC8T (59.9 s⁻¹) and ZnPEG0T (77.5 s⁻¹) (Figures S8–S10 in the Supporting Information). Because both ZnPEG8T and ZnC8T share the same primary and second coordination spheres, this huge activity difference signifies the importance of higher-sphere environments, which are rarely reported.

CV studies of both ZnC8T and ZnPEG8T with cumulative addition of water were performed to probe reaction kinetics.^[19] In the water concentration range of 1-5 m, catalyst ZnPEG8T demonstrated a higher catalytic response to available protons than ZnC8T, having a current increase at -2.4 V vs. Fc/Fc+ double that of ZnC8T (Figure 4). A KIE study using H₂O and D₂O was performed for both catalysts. As the D₂O concentration was increased, the current increased for both ZnPEG8T and ZnC8T (Figures S11 and S12 in the Supporting Information), showing a similar trend for H₂O addition. The linear dependence of the normalized catalytic current (i_{cat}/i_p) with $H_2O/$ D₂O concentration showed a nearly identical slope for both isotopes (Figure 4A, B, insets). Both ZnPEG8T and ZnC8T showed no significant isotopic difference between hydrogen and deuterium, signifying that protonation of Zn-bound CO2 is not the rate-limiting step of the CO₂ reduction process. This observation is significantly different from that of many other molecular catalytic systems, for which there is an observable

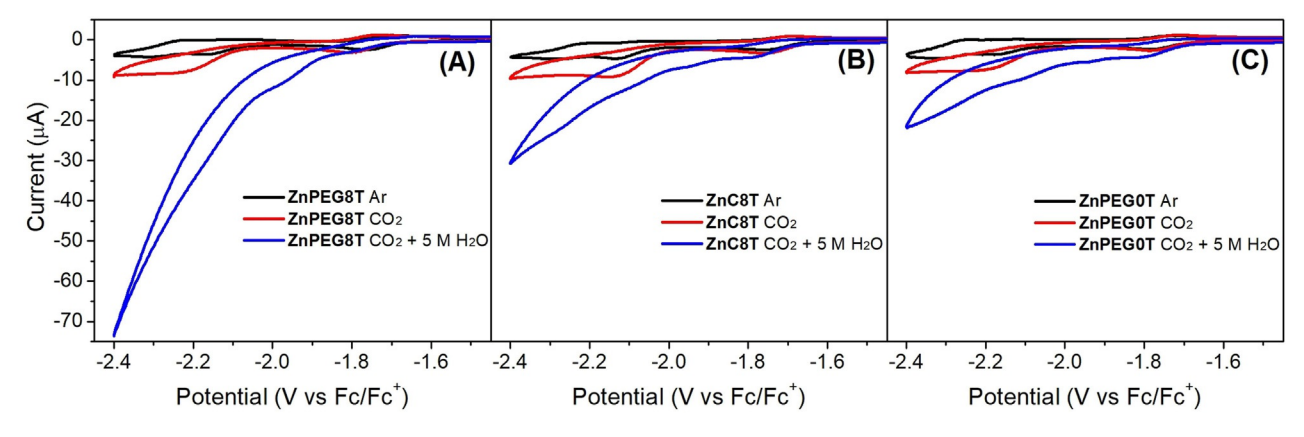
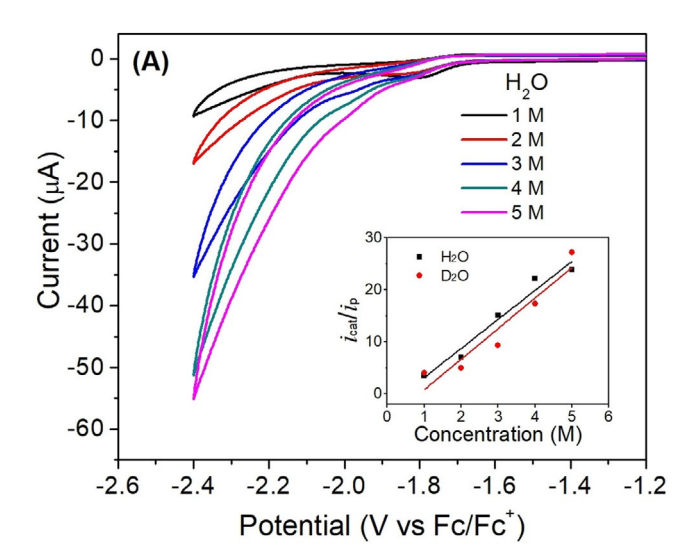


Figure 3. CVs of (A) ZnPEG8T, (B) ZnC8T, and (C) ZnPEG0T in Ar (black), saturated CO2 (red), and saturated CO2 with 5 M water (blue).

difference in the reaction rates of catalytic systems in the presence of H_2O versus D_2O . [4a,15,20] The activity difference between the two catalysts originates from their distinct architectures.



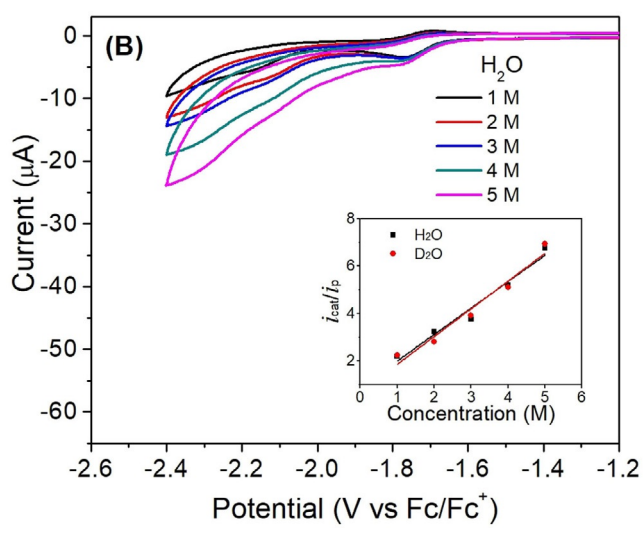


Figure 4. CVs of (A) **ZnPEG8T** and (B) **ZnC8T** with increasing amounts of $\rm H_2O$ in $\rm CO_2$ -saturated DMF with 0.1 M TBAPF₆. Inset: linear dependence of $i_{\rm cat}/i_{\rm p}$ on water concentration.

The hydrophilic PEG pocket of **ZnPEG8T** promotes relay proton shuttling to the second coordination sphere, namely the triazole bundle, for faster proton replenishment compared with that of **ZnC8T**, which has a hydrophobic pocket in which proton shuttling is inhibited. As depicted in Figure 5 A, the metal center and surrounding porphyrin ring constitute the primary coordination sphere (green area), and the second coordination sphere consists of four triazole units on each side (blue cylinder). Proton-shuttling channels (red cylinders) provide protons in a relay manner to the catalytic center for protonation of the intermediate. The observation validates the importance of employing higher functional spheres for enhanced proton-coupled reactions through installation of a hydrophilic proton channel in close proximity to the primary and second coordination sphere environments.

The selectivity and efficiency of CO₂ reduction by ZnPEG8T, ZnC8T, and the triazole-free analogue ZnPEG0T were compared by using controlled-potential electrolysis (CPE). Carbon monoxide (CO) was generated at potentials as low as -1.9 Vvs. Fc/Fc⁺. As more negative potentials were applied, the current and faradaic efficiency increased for all three compounds (Figure 5). Although both ZnPEG8T and ZnC8T catalysts were able to reach faradaic efficiencies of 100% for the production of CO at -2.4 V vs. Fc/Fc⁺, the current density of **ZnPEG8T** was far higher than that of ZnC8T (Figure 5) at all potentials studied. ZnPEG0T was the least active catalyst out of the group owing to its lack of a second coordination sphere. The stability of each catalyst was analyzed by using UV/Vis spectroscopy on the post-catalysis solutions. No difference in the Soret peak was observed for any of the catalysts, indicating the absence of demetallation during CPE (Figures S13-S15 in the Supporting Information). Spectral signatures in the Q-band region showed the possibility of stable intermediates for catalysts ZnPEG8T and ZnC8T (Figures S13 and S14 in the Supporting Information, inset). No liquid products were detected in any of the CPE measurements (Figures S16-S18 in the Supporting Information). Bare carbon paper was tested under the same CPE conditions to confirm that the system in the absence of catalyst provided a negative result. Without catalyst, the system had a very low current density (0.5 mAcm⁻²) and fara-

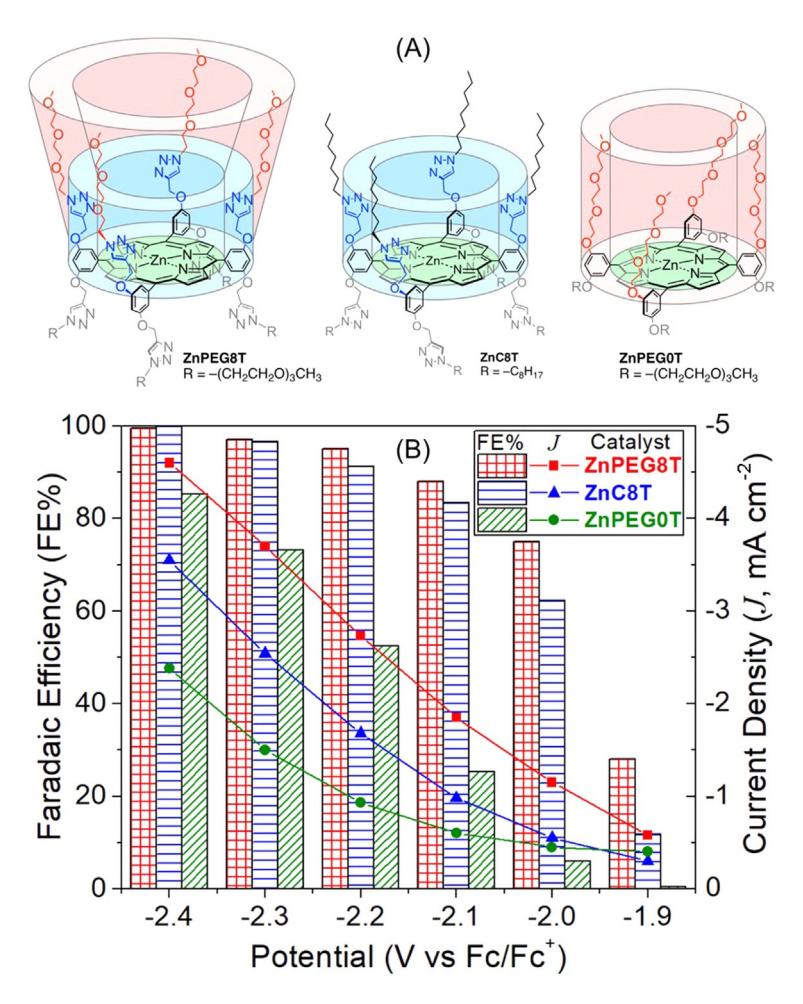


Figure 5. (A) Schematic depicting the coordination sphere environments of **ZnPEG8T**, **ZnC8T**, and **ZnPEG0T**. (B) CO faradaic efficiencies (FE%) and current densities (*J*) at various potentials for compounds **ZnPEG8T**, **ZnC8T**, and **ZnPEG0T**. H₂ gas was the only other product observed when the FE% is not 100%.

daic efficiency (37% at -2.4 V vs. Fc/Fc⁺) (Figure S19 in the Supporting Information).

The activity difference between catalysts ZnPEG8T and ZnC8T during CPE further confirms the observation in CV that higher activity originates from higher functional spheres of the complexes. The hydrophilic channel of the higher functional sphere of the Znporphyrin complex plays a significant role in proton replenishment for CO2 reduction. Although nitrogen atoms within the triazole units are the critical parts for hydration of CO2 in this reaction, the ability of those protons to be replenished is influenced by the higher functional sphere. The PEG units in ZnPEG8T create a more hydrophilic environment around the primary (Zn center) and second (triazole bundle) coordination spheres to facilitate proton replenishment, which subsequently provides more protons to the reduction reaction. The inferior activity of ZnPEG0T suggests a synergistic effect between the hydrophilic proton channel and second coordination sphere for CO_2 conversion. Because zinc is a d_{10} transition metal, it is redox innocent and only participates as the CO₂ binding site. The electron transfer that is necessary for CO2 reduction is facilitated by the redox-active porphyrin ligand.^[21]

The catalytic efficiencies of the **ZnPEG8T**, **ZnC8T**, and **ZnPEG0T** catalysts were benchmarked using the methods of Savéant and co-workers to provide Tafel plots (Figure 6)^[18b] that present TOF as a function of overpotential. This method is independent of many experimental conditions, such as cell configuration and size, and only accounts for the activity of the catalysts in the diffusion layer; therefore, it reflects intrinsic catalytic activity. The **ZnPEG8T** catalyst was the most active of the three catalysts. For a comparison

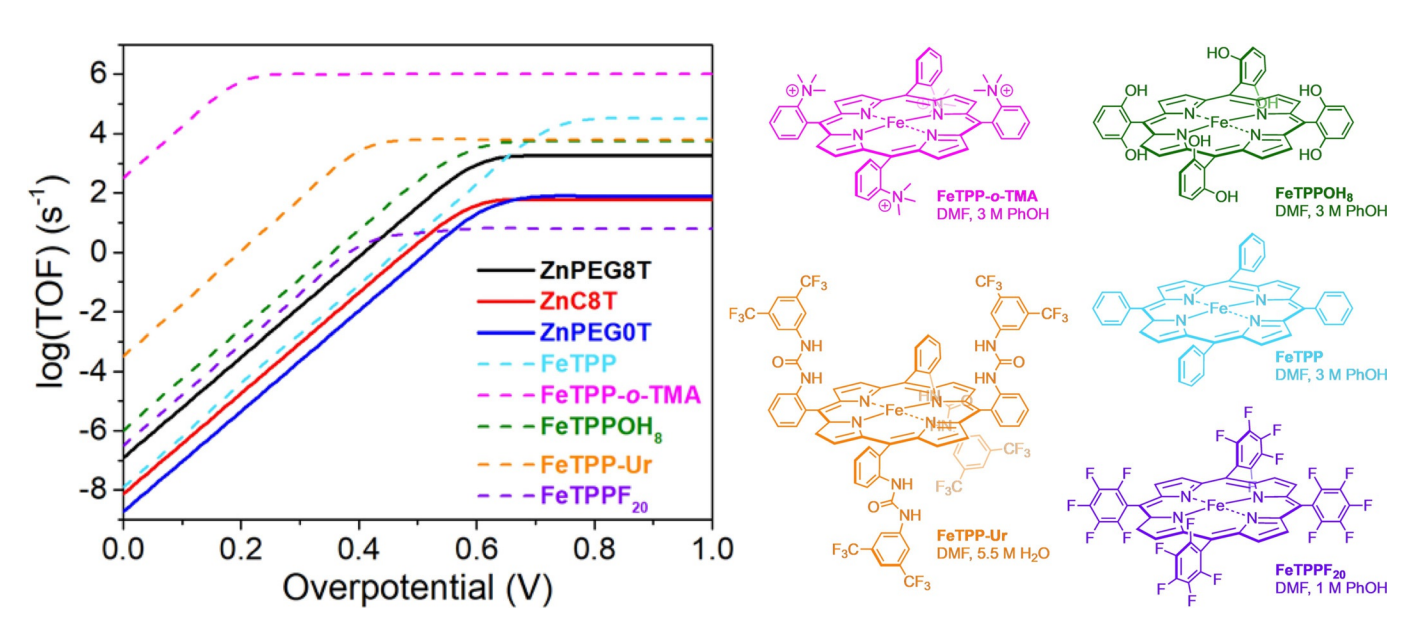


Figure 6. Tafel plots derived from CVs of ZnPEG8T, ZnC8T, and ZnPEG0T in DMF with 5 M H₂O. Data for FeTPP-o-TMA, FeTPPOH₈, and FeTPPF₂₀ were derived from Savéant and co-workers. [7,21] Data for FeTPP-Ur in DMF with 5.5 M H₂O was derived from Aukauloo and co-workers. [4d]



with several extensively studied iron porphyrin catalysts, ^[4d] we plotted our catalysts against five iron porphyrin catalysts, including two without a higher coordination sphere [iron tetraphenylporphyrin (FeTPP)^[7] and iron tetra(pentafluorophenyl)-porphyrin (FeTPF₂₀)^[22b] and three bearing trimethyl ammonium (FeTPP-o-TMA)^[7], hydroxyl (FeTPPOH₈)^[22a], and urea (FeTPP-Ur)^[4d] as their second coordination spheres. The existence of a second coordination sphere provided a decrease in overpotential. To be compared to the zinc complexes, FeTPP-Ur^[4d] utilizes a multipoint hydrogen-bonding network to transfer protons to the metal center. The catalyst Fe-o-TMA adopted a through-space mechanism by positive charges on the second coordination sphere to stabilize the CO₂-bound intermediate.^[7]

In conclusion, the catalytic activities and efficiencies of three structurally distinct Zn-porphyrin complexes were studied to probe the structure-function relationship of electrocatalytic CO₂ reduction. CV and CPE studies indicated that catalyst ZnPEG8T showed a thirty times greater activity level than that of analogous catalysts ZnC8T and ZnPEG0T. KIE studies showed no significant differences for H₂O versus D₂O, revealing that protons are not involved in the rate-limiting step, which is significantly different from other reported molecular systems. Compared to the PEG-free catalyst ZnC8T, the highly polar chains of the ZnPEG8T catalyst functioned as a hydrophilic proton shuttling channel, providing faster proton relay to the second coordination sphere (triazole bundle) for continuous protonation of the metallocarboxylate intermediate. This strategy can be directly extended to other proton-coupled transformations, such as water oxidation, oxygen reduction, and methane oxidation.[16]

Acknowledgements

The authors acknowledge the University of Cincinnati for startup funding support. NMR experiments were performed on a Bruker AVANCE NEO 400 MHz NMR spectrometer funded by NSF-MRI arant CHE-1726092.

Conflict of interest

The authors declare no conflict of interest.

Keywords: CO_2 reduction \cdot coordination sphere \cdot homogeneous catalysis \cdot proton transport \cdot redox-active ligand

- a) M. L. Helm, M. P. Stewart, R. M. Bullock, M. R. DuBois, D. L. DuBois, Science 2011, 333, 863–866; b) D. L. DuBois, Inorg. Chem. 2014, 53, 3935–3960; c) L. Kohler, J. Niklas, R. C. Johnson, M. Zeller, O. G. Poluektov, K. L. Mulfort, Inorg. Chem. 2019, 58, 1697–1709; d) M. D. Doud, K. A. Grice, A. M. Lilio, C. S. Seu, C. P. Kubiak, Organometallics 2012, 31, 779–782; e) A. Rana, B. Mondal, P. Sen, S. Dey, A. Dey, Inorg. Chem. 2017, 56, 1783–1793.
- [2] a) S. Sahu, D. P. Goldberg, J. Am. Chem. Soc. 2016, 138, 11410-11428;
 b) C. T. Carver, B. D. Matson, J. M. Mayer, J. Am. Chem. Soc. 2012, 134, 5444-5447;
 c) S. Samanta, K. Sengupta, K. Mittra, S. Bandyopadhyay, A. Dey, Chem. Commun. 2012, 48, 7631-7633.

- [3] B. R. Galan, J. Schöffel, J. C. Linehan, C. Seu, A. M. Appel, J. A. S. Roberts, M. L. Helm, U. J. Kilgore, J. Y. Yang, D. L. DuBois, C. P. Kubiak, J. Am. Chem. Soc. 2011, 133, 12767 – 12779.
- [4] a) S. Roy, B. Sharma, J. Pecaut, P. Simon, M. Fontecave, P. D. Tran, E. Derat, V. Artero, J. Am. Chem. Soc. 2017, 139, 3685 3696; b) A. Chapovetsky, T. H. Do, R. Haiges, M. K. Takase, S. C. Marinescu, J. Am. Chem. Soc. 2016, 138, 5765 5768; c) C. Costentin, S. Drouet, M. Robert, J. M. Savéant, Science 2012, 338, 90 94; d) P. Gotico, B. Boitrel, R. Guillot, M. Sircoglou, A. Quaranta, Z. Halime, W. Leibl, A. Aukauloo, Angew. Chem. Int. Ed. 2019, 58, 4504 4509; Angew. Chem. 2019, 131, 4552 4557; e) J. Agarwal, T. W. Shaw, H. F. Schaefer Ill, A. B. Bocarsly, Inorg. Chem. 2015, 54, 5285 5294; f) S. Sung, X. Li, L. M. Wolf, J. R. Meeder, N. S. Bhuvanesh, K. A. Grice, J. A. Panetier, M. Nippe, J. Am. Chem. Soc. 2019, 141, 6569 6582; g) B. Mondal, A. Rana, P. Sen, A. Dey, J. Am. Chem. Soc. 2015, 137, 11214 11217; h) S. Sung, D. Kumar, M. Gil-Sepulcre, M. Nippe, J. Am. Chem. Soc. 2017, 139, 13993 13996.
- [5] J. Rosenthal, D. G. Nocera, Acc. Chem. Res. 2007, 40, 543-553.
- [6] a) C. G. Margarit, C. Schnedermann, N. G. Asimow, D. G. Nocera, Organometallics 2019, 38, 1219 – 1223; b) C. Costentin, G. Passard, M. Robert, J. M. Savéant, J. Am. Chem. Soc. 2014, 136, 11821 – 11829.
- [7] I. Azcarate, C. Costentin, M. Robert, J. M. Savéant, J. Am. Chem. Soc. 2016, 138, 16639 – 16644.
- [8] B. P. Sullivan, C. M. Bolinger, D. Conrad, W. J. Vining, T. J. Meyer, J. Chem. Soc. Chem. Commun. 1985, 1414–1416.
- [9] a) P. Kang, Z. Chen, M. Brookhart, T. J. Meyer, Top. Catal. 2015, 58, 30-45; b) Y. Y. Birdja, J. Shen, M. T. M. Koper, Catal. Today 2017, 288, 37-47; c) J. M. Barlow, J. Y. Yang, ACS Cent. Sci. 2019, 5, 580-588; d) J. Qiao, Y. Liu, F. Hong, J. Zhang, *Chem. Soc. Rev.* **2014**, *43*, 631–675; e) S. Lin, C. S. Diercks, Y. B. Zhang, N. Kornienko, E. M. Nichols, Y. Zhao, A. R. Paris, D. Kim, P. Yang, O. M. Yaghi, C. J. Chang, Science 2015, 349, 1208-1213; f) M. Abdinejad, A. Seifitokaldani, C. Dao, E. H. Sargent, X.-A. Zhang, H. B. Kraatz, ACS Appl. Energy Mater. 2019, 2, 1330-1335; g) J. Langer, A. Hamza, I. Pápai, Angew. Chem. Int. Ed. 2018, 57, 2455 - 2458; Angew. Chem. 2018, 130, 2480 - 2483; h) C. Costentin, M. Robert, J. M. Savéant, Acc. Chem. Res. 2015, 48, 2996 - 3006; i) C. I. Shaughnessy, D. J. Sconyers, T. A. Kerr, H. J. Lee, B. Subramaniam, K. C. Leonard, J. D. Blakemore, ChemSusChem 2019, 12, 3761-3768; j) R. Francke, B. Schille, M. Roemelt, Chem. Rev. 2018, 118, 4631-4701; k) A. M. Appel, J. E. Bercaw, A. B. Bocarsly, H. Dobbek, D. L. DuBois, M. Dupuis, J. G. Ferry, E. Fujita, R. Hille, P. J. Kenis, C. A. Kerfeld, R. H. Morris, C. H. Peden, A. R. Portis, S. W. Ragsdale, T. B. Rauchfuss, J. N. Reek, L. C. Seefeldt, R. K. Thauer, G. L. Waldrop, Chem. Rev. 2013, 113, 6621-6658; I) A. Goeppert, M. Czaun, J. P. Jones, G. K. Surya Prakash, G. A. Olah, Chem. Soc. Rev. 2014, 43, 7995-8048; m) B. J. McNicholas, J. D. Blakemore, A. B. Chang, C. M. Bates, W. W. Kramer, R. H. Grubbs, H. B. Gray, J. Am. Chem. Soc. 2016, 138, 11160 - 11163; n) E. Haviv, D. Azaiza-Dabbah, R. Carmieli, L. Avram, J. M. L. Martin, R. Neumann, J. Am. Chem. Soc. 2018, 140, 12451 – 12456; o) Z. Weng, Y. Wu, M. Wang, J. Jiang, K. Yang, S. Huo, X. F. Wang, Q. Ma, G. W. Brudvig, V. S. Batista, Y. Liang, Z. Feng, H. Wang, Nat. Commun. 2018, 9, 415; p) Z. Weng, J. Jiang, Y. Wu, Z. Wu, X. Guo, K. L. Materna, W. Liu, V. S. Batista, G. W. Brudvig, H. Wang, J. Am. Chem. Soc. 2016, 138, 8076 - 8079; q) J. Jiang, A. J. Matula, J. R. Swierk, N. Romano, Y. Wu, V. S. Batista, R. H. Crabtree, J. S. Lindsey, H. Wang, G. W. Brudvig, ACS Catal. 2018, 8, 10131 - 10136; r) S. A. Chabolla, C. W. Machan, J. Yin, E. A. Dellamary, S. Sahu, N. C. Gianneschi, M. K. Gilson, F. A. Tezcan, C. P. Kubiak, Faraday Discuss. 2017, 198, 279-300; s) J. D. Froehlich, C. P. Kubiak, J. Am. Chem. Soc. 2015, 137, 3565-3573; t) A. Zhanaidarova, S. C. Jones, E. Despagnet-Ayoub, B. R. Pimentel, C. P. Kubiak, J. Am. Chem. Soc. 2019, 141, 17270 - 17277; u) B. Mondal, P. Sen, A. Rana, D. Saha, P. Das, A. Dey, ACS Catal. 2019, 9, 3895-3899; v) P. Sen, B. Mondal, D. Saha, A. Rana, A. Dey, Dalton Trans. 2019, 48, 5965 - 5977; w) A. Singha, K. Mittra, A. Dey, Dalton Trans. 2019, 48, 7179-7186; x) A. W. Nichols, C. W. Machan, Front. Chem. 2019, 7, 397; y) S. L. Hooe, J. M. Dressel, D. A. Dickie, C. W. Machan, ACS Catal. 2020, 10, 1146-1151; z) C. Jiang, A. W. Nichols, C. W. Machan, Dalton Trans. 2019, 48, 9454-9468; aa) M. Yousif, A. C. Cabelof, P. D. Martin, R. L. Lord, S. Groysman, Dalton Trans. 2016, 45, 9794-9804; ab) R. Narayanan, M. McKinnon, B. R. Reed, K. T. Ngo, S. Groysman, J. Rochford, Dalton Trans. 2016, 45, 15285-15289; ac) D. J. Sconyers, C. I. Shaughnessy, H. J. Lee, B. Subramaniam, K. C. Leonard, J. Blakemore, ChemSusChem 2020, DOI: https://doi.org/10.1002/



- cssc.202000390; ad) D. Sun, X. Xu, Y. Qin, S. P. Jiang, Z. Shao, *ChemSusChem* **2020**, *13*, 39–58.
- [10] a) E. M. Nichols, J. S. Derrick, S. K. Nistanaki, P. T. Smith, C. J. Chang, Chem. Sci. 2018, 9, 2952 – 2960; b) K. Guo, X. Li, H. Lei, W. Zhang, R. Cao, ChemCatChem 2020, 12, 1591 – 1595.
- [11] a) S. Ringe, E. L. Clark, J. Resasco, A. Walton, B. Seger, A. T. Bell, K. Chan, Energy Environ. Sci. 2019, 12, 3001–3014; b) M. König, J. Vaes, E. Klemm, D. Pant, iScience 2019, 19, 135–160; c) B. Zhao, H. Lei, N. Wang, G. Xu, W. Zhang, R. Cao, Chem. Eur. J. 2020, 26, 4007–4012.
- [12] U. O. Nwabara, E. R. Cofell, S. Verma, E. Negro, P. J. A. Kenis, *ChemSusChem* **2020**, *13*, 855–875.
- [13] a) A. Dutta, S. Lense, J. A. S. Roberts, M. L. Helm, W. J. Shaw, Eur. J. Inorg. Chem. 2015, 5218–5225; b) B. Ginovska-Pangovska, A. Dutta, M. L. Reback, J. C. Linehan, W. J. Shaw, Acc. Chem. Res. 2014, 47, 2621–2630.
- [14] A. Lashgari, C. K. Williams, J. L. Glover, Y. Wu, J. Chai, J. Jiang, 2020, unpublished results.
- [15] A. Chapovetsky, M. Welborn, J. M. Luna, R. Haiges, T. F. Miller III, S. C. Marinescu, ACS Cent. Sci. 2018, 4, 397 404.
- [16] a) K. J. Lee, J. L. Dempsey, ACS Energy Lett. 2018, 3, 2477 2479; b) D. R. Weinberg, C. J. Gagliardi, J. F. Hull, C. F. Murphy, C. A. Kent, B. C. Westlake, A. Paul, D. H. Ess, D. G. McCafferty, T. J. Meyer, Chem. Rev. 2012, 112, 4016 4093.
- [17] J. Schneider, H. Jia, J. T. Muckerman, E. Fujita, Chem. Soc. Rev. 2012, 41, 2036–2051.

- [18] a) E. S. Rountree, B. D. McCarthy, T. T. Eisenhart, J. L. Dempsey, *Inorg. Chem.* 2014, 53, 9983–10002; b) C. Costentin, S. Drouet, M. Robert, J. M. Savéant, J. Am. Chem. Soc. 2012, 134, 11235–11242; c) N. Elgrishi, K. J. Rountree, B. D. McCarthy, E. S. Rountree, T. T. Eisenhart, J. L. Dempsey. J. Chem. Educ. 2018, 95, 197–206.
- [19] a) S. El Ghachtouli, B. Lassalle-Kaiser, P. Dorlet, R. Guillot, E. Anxolabéhère-Mallart, C. Costentin, A. Aukauloo, *Energy Environ. Sci.* 2011, 4, 2041–2044; b) S. C. Sawant, X. Wu, J. Cho, K. B. Cho, S. H. Kim, M. S. Seo, Y. M. Lee, M. Kubo, T. Ogura, S. Shaik, W. Nam, *Angew. Chem. Int. Ed.* 2010, 49, 8190–8194; *Angew. Chem.* 2010, 122, 8366–8370.
- [20] a) Y. Liu, C. C. L. McCrory, Nat. Commun. 2019, 10, 1683; b) S. Fukuzumi, Y. M. Lee, H. S. Ahn, W. Nam, Chem. Sci. 2018, 9, 6017 – 6034.
- [21] a) S. El Ghachtouli, B. Lassalle-Kaiser, R. Guillot, A. Aukauloo, Eur. J. Inorg. Chem. 2014, 4750–4755; b) O. R. Luca, R. H. Crabtree, Chem. Soc. Rev. 2013, 42, 1440–1459; c) Y. Wu, J. Jiang, Z. Weng, M. Wang, D. L. J. Broere, Y. Zhong, G. W. Brudvig, Z. Feng, H. Wang, ACS Cent. Sci. 2017, 3, 847–852.
- [22] a) C. Costentin, G. Passard, M. Robert, J. M. Savéant, *Proc. Natl. Acad. Sci. USA* **2014**, *111*, 14990 14994; b) I. Azcarate, C. Costentin, M. Robert, J.-M. Savéant, *J. Phys. Chem. C* **2016**, *120*, 28951 28960.

Manuscript received: April 21, 2020 Accepted manuscript online: May 7, 2020 Version of record online: June 5, 2020